



Fermi National Accelerator Laboratory

FERMILAB-Pub-77/29-EXP

7200.311

(Submitted to Phys. Rev. Lett.)

EXPERIMENTAL EVIDENCE FOR THE GENERAL THEOREM
IN 100 GeV/c $\bar{p}p$ INTERACTIONS

Rajendran Raja

Fermi National Accelerator Laboratory, Batavia, Illinois 60510

March 1977



EXPERIMENTAL EVIDENCE FOR THE GENERAL THEOREM
IN 100 GEV/C $\bar{p}p$ INTERACTIONS

BY

Rajendran Raja
Fermi National Accelerator Laboratory,
Batavia, Illinois 60510, U.S.A

March 1977

ABSTRACT

We present experimental evidence for the general theorem on inclusive reactions¹ in 100 GeV/c $\bar{p}p$ interactions. The agreement between the predictions of the theorem and the data is remarkable in all areas of phase space.

In reference 1, I showed from general considerations, that the ratio of the invariant single particle inclusive cross section of a subset to that of the whole set is a function of M^2 , the missing mass squared of the recoiling system, only and not of s and t . The result holds for each point in phase space and at all energies. In this paper we present experimental evidence for the theorem for the channel $\bar{p}p \rightarrow \pi^+X$ at $\sqrt{s} = 100$ GeV/c. We have used only tracks that go backward in the center of mass system. Backward going π^- 's were reflected in the center of mass and treated as forward going π^+ 's, a procedure valid owing to C-invariance. The data were obtained from the 30" bubble chamber/wide-gap spark chamber hybrid system at Fermilab and consist of 23,983 equivalent π^+ tracks. Protons of momentum less than 1.4 GeV/c were removed by using ionization information. Protons with momentum greater than 1.4 GeV/c were corrected for by demanding a flat proton Feynman x distribution till $x = -0.2$ and an exponentially decaying x distribution for $x > -0.2$ of slope 4.8. This is the behaviour observed for Λ^0 's in this experiment³ and we assume that protons being baryons will show a similar fall off with x . We estimate an overall K^+ contamination of 6% but have not corrected for this since we are essentially interested in ratios of cross sections obtained in the same experiment.

Figure 1(a) shows the M^2 distribution for overall data, for the subset possessing primary multiplicity 2,4 or 6 (subset I) and for the subset possessing primary multiplicity 12,14 or 16 (subset II). The M^2 distributions for the two subsets differ greatly in shape. Figure 1(b) shows the t distribution for overall data and subsets I and II, t being defined as the momentum transfer squared between the target proton and the outgoing pion. The three t distributions also differ greatly in shape.

Figure 2 is a plot of the ratio of $d\sigma/dM^2$ for subsets I, II to $d\sigma/dM^2$ overall as functions of M^2 . We denote these functions $\alpha_I(M^2)$ and $\alpha_{II}(M^2)$, the subscript denoting the subset involved. The full curves are fits to the data of a 3rd order polynomial in M^2 . The general theorem holds that

$$\frac{C(M^2, s, t)}{B(M^2, s, t)} = \alpha(M^2)$$

where B,C are the invariant cross sections for overall data and a subset respectively. This implies that if each event is given a weight $\alpha(M^2)$, the overall data should mimic the subset at all points in phase space. In what follows, we will compare the inclusive cross sections for subsets I and II with overall data weighted by the appropriate $\alpha(M^2)$, as functions of M^2 and t .

Figure 3 shows the t distributions for subset I in various range of M^2 . Also shown are overall data weighted by $\alpha_I(M^2)$ parametrised as a cubic polynomial. The agreement between the t distributions is excellent in all ranges of M^2 . Even though the overall data has a t distribution different in shape to that of subset I, the shapes agree for all ranges of M^2 when the events are weighted by $\alpha_I(M^2)$. Figure 4 is the corresponding plot for subset II in the same ranges of M^2 . Superimposed are overall data weighted by the function $\alpha_{II}(M^2)$. The variation in shape and magnitude of the t distributions with M^2 of the subset, is faithfully reproduced by the overall data weighted by $\alpha_{II}(M^2)$.

Figure 5 shows the M^2 distribution for different ranges of t for subset I and compares it with overall data weighted by $\alpha_I(M^2)$. Figure 6 is a corresponding plot for subset II. The overall data weighted by the appropriate $\alpha(M^2)$ mimic the subset cross sections for all ranges of t . The shape of the M^2 distribution for the subset varies with t . Weighting the overall data with the appropriate $\alpha(M^2)$ reproduces these variations, as required by the general theorem.

Figure 7 illustrates a test of Lemma 2 of the general theorem¹, which states that $C_1/B_1 = C_2/B_2 = \alpha(M^2)$, where C_1 and B_1 are the inclusive cross sections for the subset

and overall data for the channel $\bar{p}p \rightarrow \pi^+X$ and C_2 and B_2 are the corresponding quantities for the channel $\bar{p}p \rightarrow \pi^-X$. We have used π^+ and π^- data from the backward center of mass hemisphere. The agreement is excellent for subsets I and II. Superimposed are the cubic fits to $\alpha_I(M^2)$ and $\alpha_{II}(M^2)$, which lie on top of the data as required by lemma 2.

The author has tested the subset possessing primary multiplicity 8 or 10. The α function for this subset is more or less flat with M^2 . The agreement between the overall data weighted by $\alpha(M^2)$ and the subset data is equally good but we omit presentation of these data owing to space limitations.

To conclude, data for the channel $\bar{p}p \rightarrow \pi^+X$ at 100 GeV/c obey the general theorem remarkably well in all parts of phase space. The author is grateful to the Cambridge-Fermilab-MSU collaboration, particularly Lou Voyvodic, Gerry Smith and Jim Whitmore for facilitating this work.

REFERENCES

¹ 'A General Theorem for inclusive reactions', R.Raja,
Fermilab Preprint 77/28 (1977)

² We are grateful to the Cambridge-Fermilab-MSU
collaboration for making this data available.

³ 'Neutral particle production in 100 GeV/c $\bar{p}p$
interactions. Cambridge-Fermilab-MSU collaboration,
Phys.Rev.D15,(1977),627.

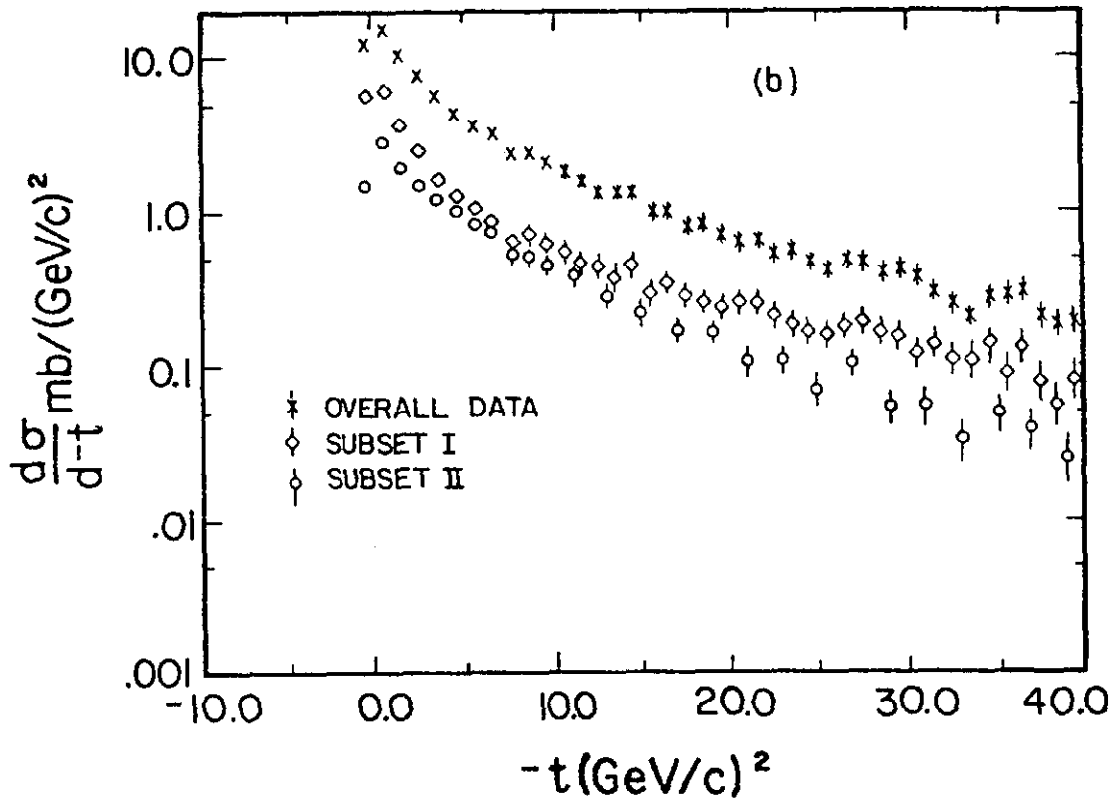
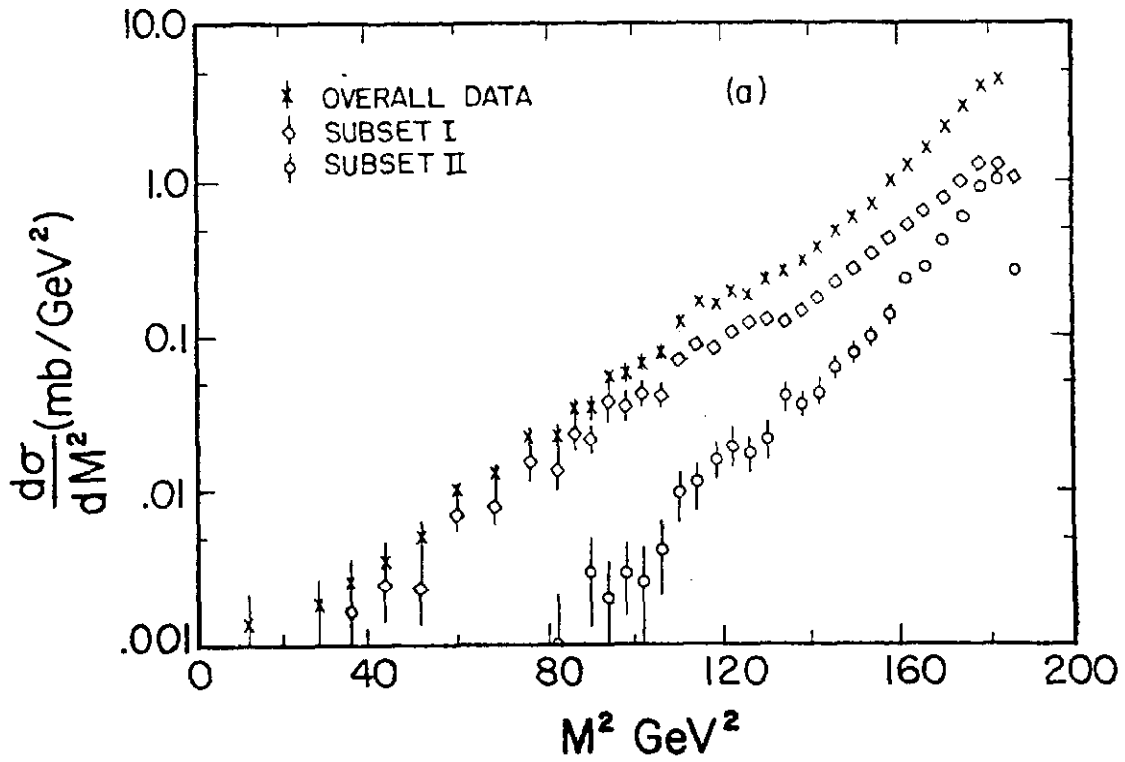


Fig. 1. (a) M^2 distributions for overall data, 2 4 and 6 prongs (subset I) and 12, 14 and 16 prongs (subset II).

Fig. 1. (b) t distribution for overall data, subset I and subset II.

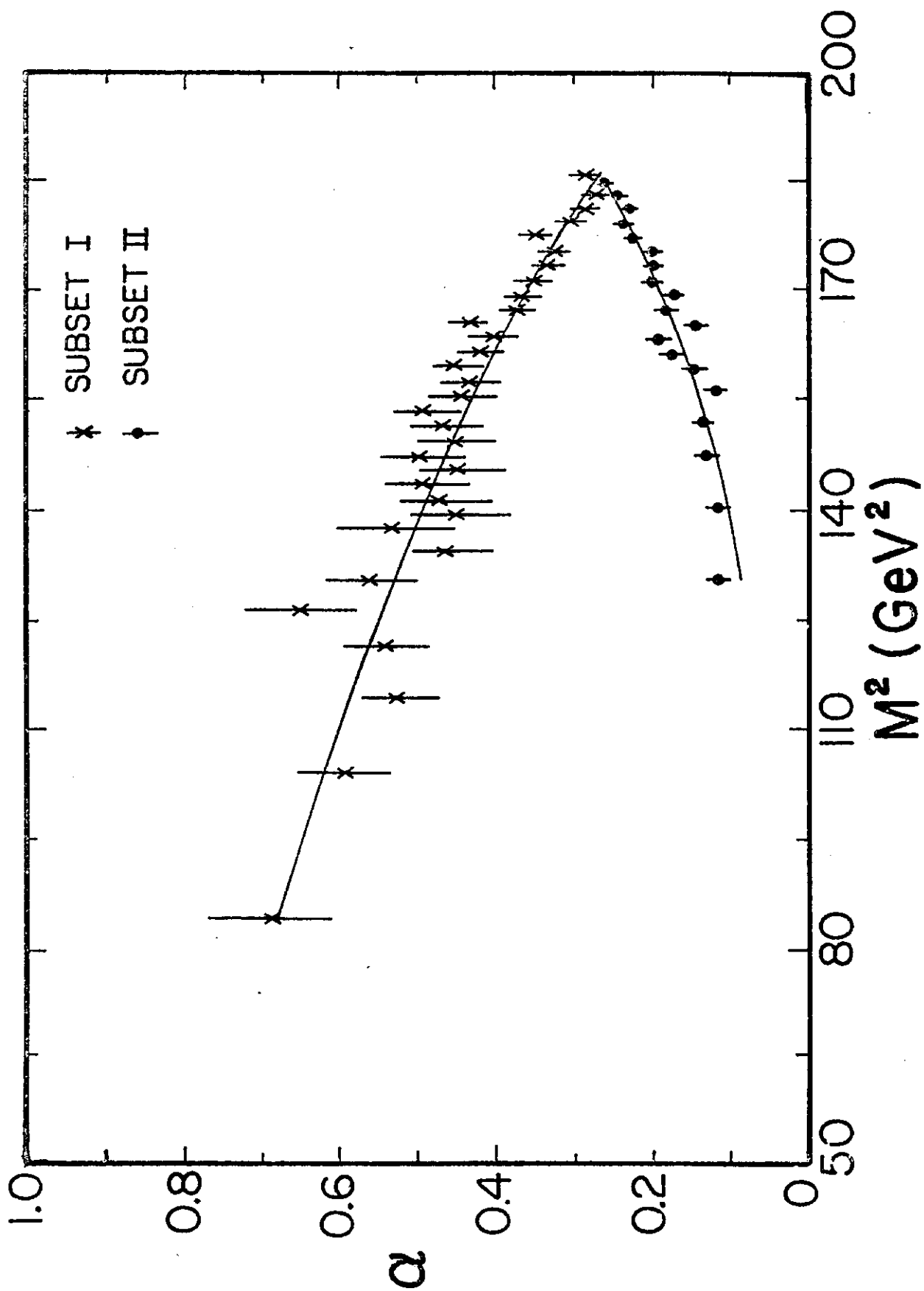


Fig. 2. Ratio of M^2 distributions of subsets I and II to overall data. Curves are fits to a cubic polynomial.

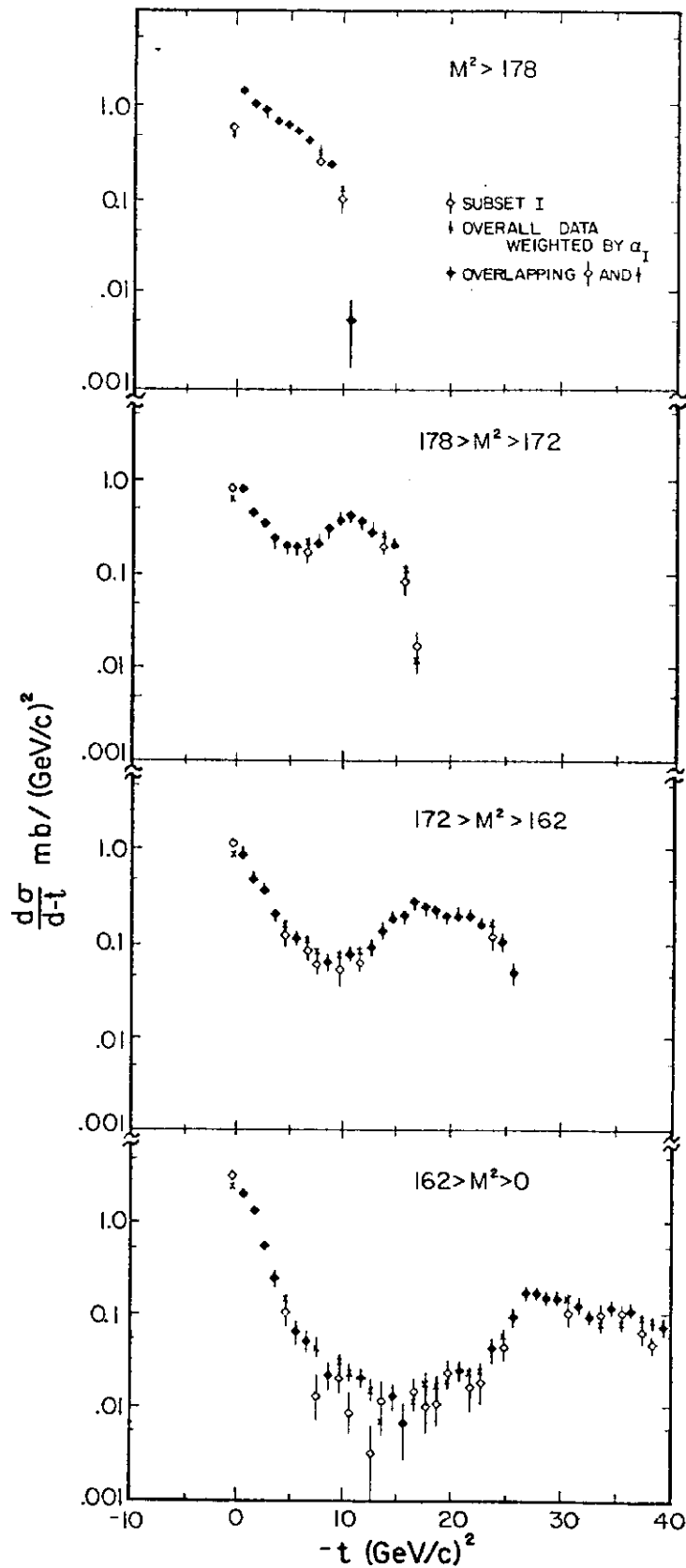


Fig. 3. Comparison of t distribution for subset I with overall data weighted by $\alpha_I(M^2)$ for various M^2 ranges.

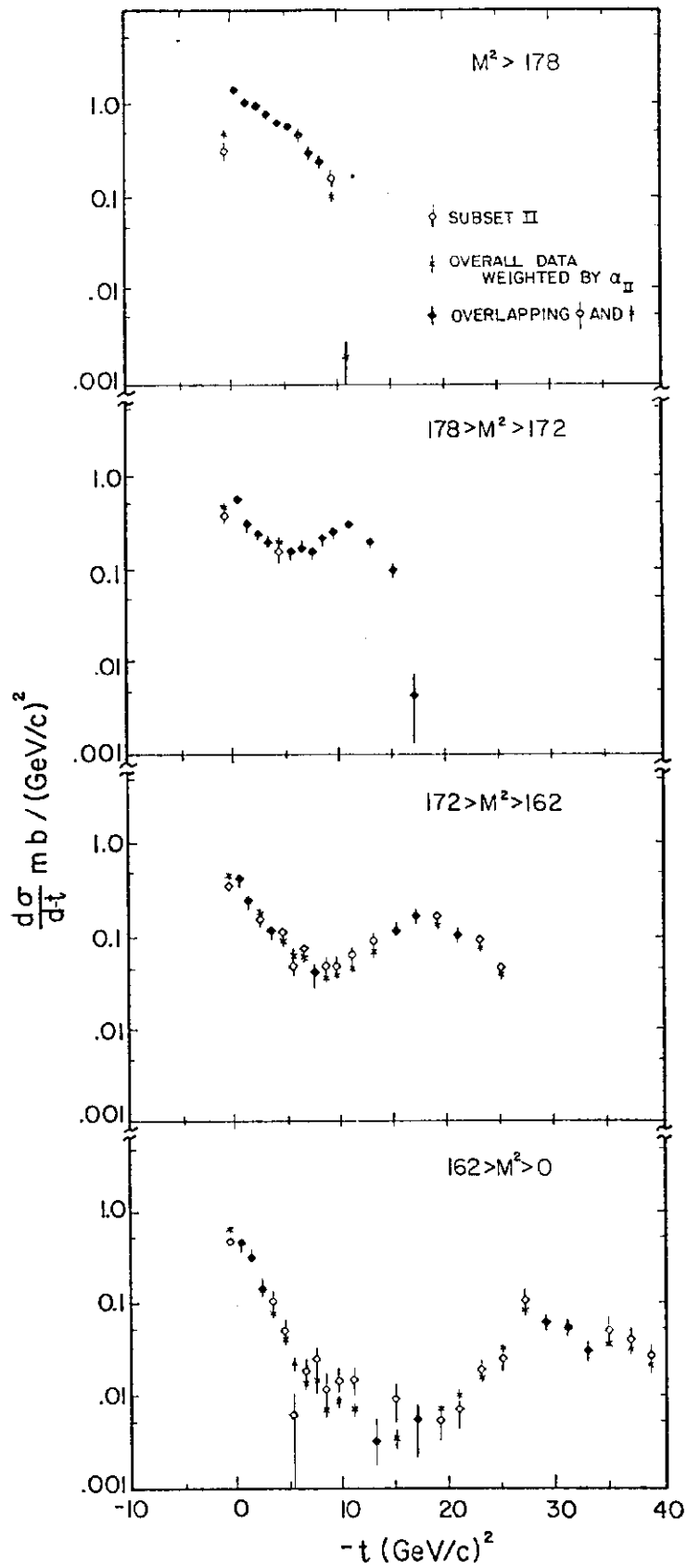


Fig. 4. Comparison of t distribution for subset II with overall data weighted by $\alpha_{II}(M^2)$ for various M^2 ranges.

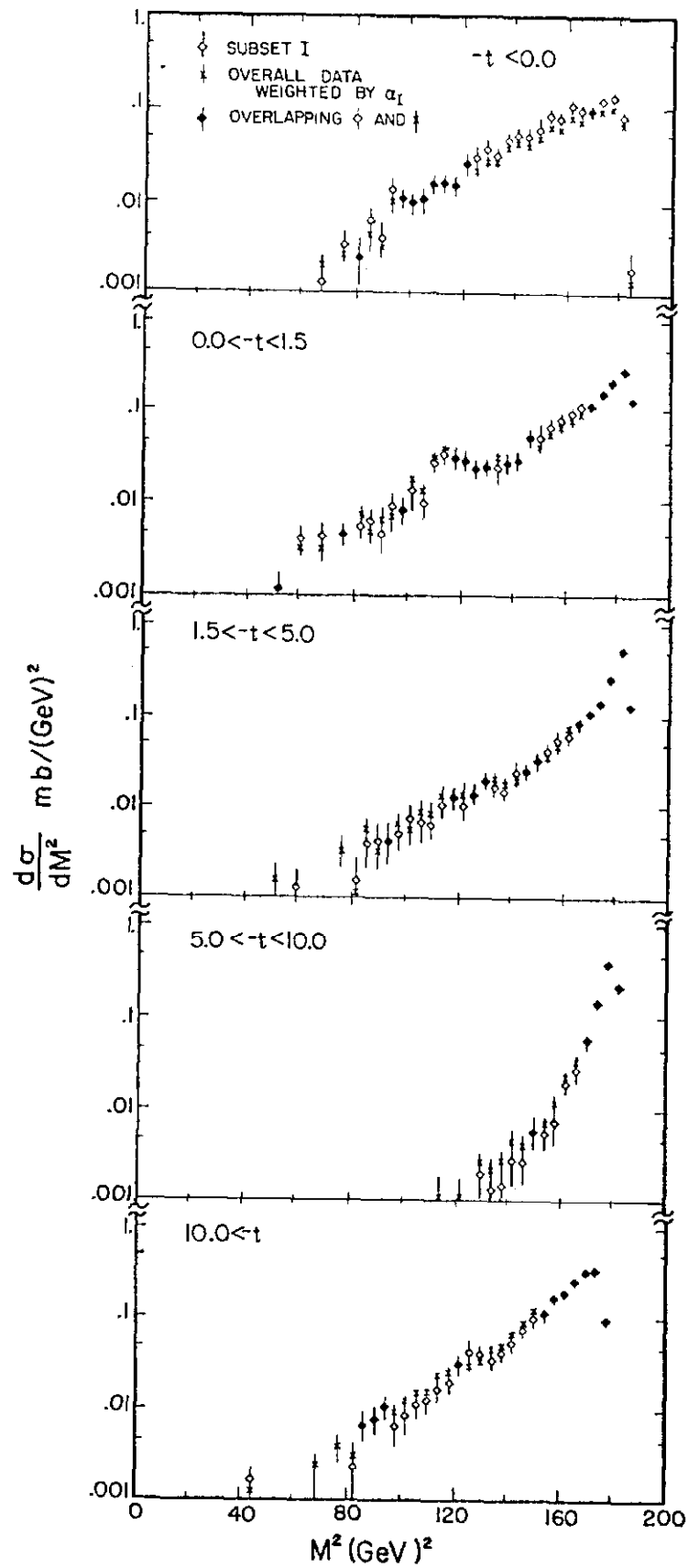


Fig. 5. Comparison of M^2 distribution for subset I with overall data weighted by $\alpha_I(M^2)$ for various t ranges.

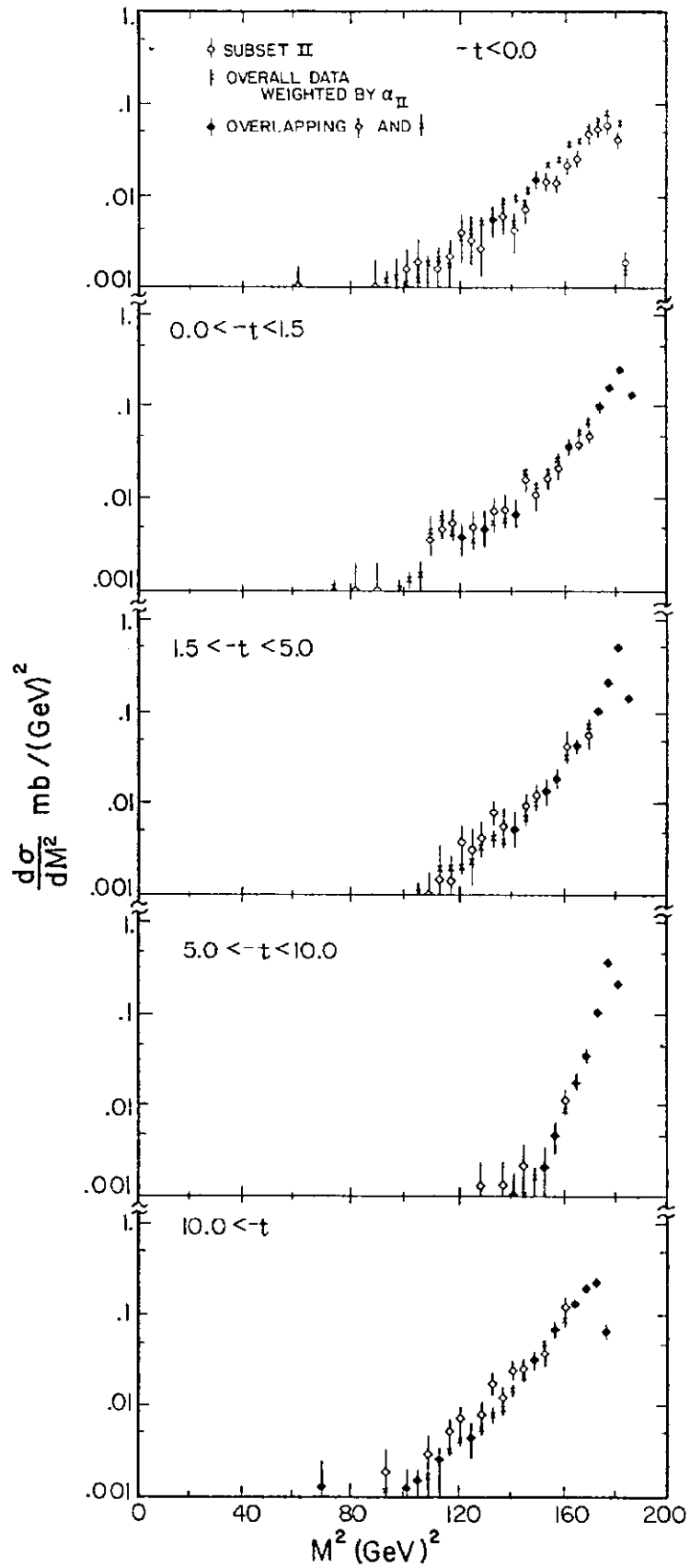


Fig. 6. Comparison of M^2 distribution for subset II with overall data weighted by $\alpha_{II}(M^2)$ for various t ranges.

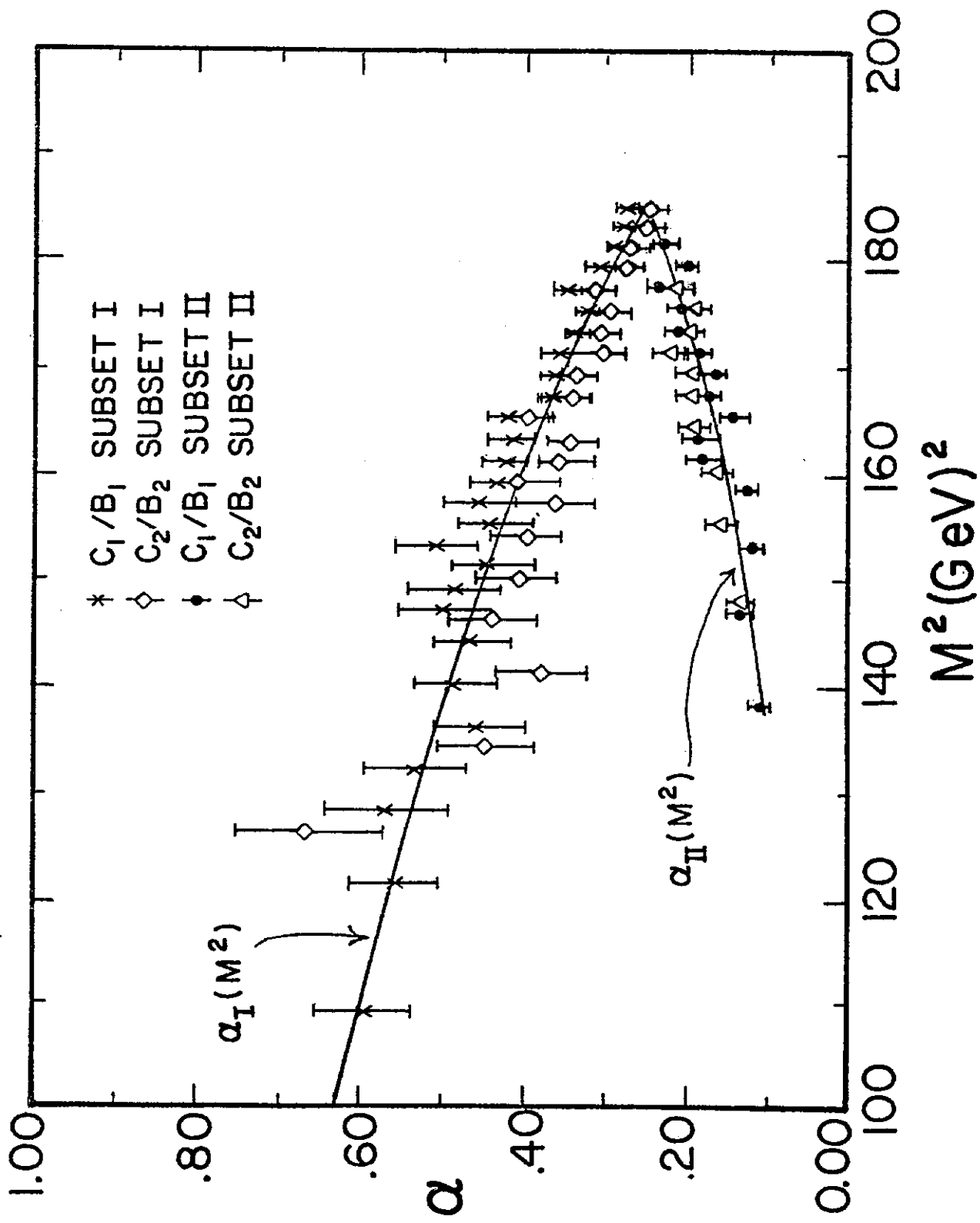


Fig. 7. Test of lemma 2 for subsets I and II. The curves are the cubic fits shown in Fig. 2.